URSI - RCRS 2022, IIT (Indore), India, 1 - 4 December, 2022

A new perspective on Aura MLS observations of stratospheric ozone distributions associated with Southern Hemisphere Sudden Stratospheric warming

Veenus Venugopal* [1, 2], and Siddarth Shankar Das [1]
(1) Space Physics Laboratory, Vikram Sarabhai Space Centre, ISRO, Thiruvananthapuram, 695022, India
(2) Department of Physics, University of Kerala, Thiruvananthapuram, 695034, India

Abstract

Brewer-Dobson circulation (BDC) carries air upwards from the tropical upper-troposphere lower stratosphere region and further towards the poles. BDC is observed to intensify during sudden stratospheric warming (SSW) events. SSWs occur frequently in the Northern Hemisphere (NH) and rarely in the Southern Hemisphere (SH). In 2002, a major SSW was recorded in the SH. Recently, an intense warming was observed in the SH on September 16, 2019. The present study focused on the recent event and analyzed the variations in the intensity of BDC and the resulting stratospheric composition following the warming. BDC metrics are evaluated using the ERA5 reanalysis products. Aura Microwave Limb Sounder (MLS) observations are used to analyze the stratospheric distribution of ozone. The Eliassen-Palm flux divergence, indicative of wave driving, is observed to be increasing before the SSW, and subsiding afterwards. The BDC circulation follows the wave driving and intensifies along the warming episode, as observed from the residual mean meridional stream function and diabatic heating rate. The resulting stratospheric distribution shows a negative ozone anomaly in the tropical upper stratosphere and a downward propagating positive anomaly in the polar stratosphere around the central dates.

1. Introduction

Brewer-Dobson circulation (BDC) carries air upwards from the tropical upper-troposphere lower stratosphere region and further towards the poles [2, 3]. BDC is driven by the momentum deposited by breaking planetary waves. Studies have shown that BDC intensity is altered during sudden stratospheric warming (SSW) events. SSWs are characterised by rapid temperature rise over the polar stratosphere in a short period of time. Temperature increase of up to 50 K was observed during extreme warming events. During major warming, along with the temperature increase, the zonal-mean zonal wind reverses, changing the dynamical background for planetary wave propagation. Thus, the wave-driven circulation, BDC, undergoes sub-seasonal variations during SSWs.

A few studies have analyzed the changes in BDC during SSW events. Tao et al., [10] have analyzed the variation in BDC during three major SSWs to show that the deep branch of BDC intensifies around the central date and the shallow branch accelerates after the central date. de la Cámara et al., [4] have studied the response of the stratospheric transport and isentropic mixing using ERA Interim reanalysis and model simulations to show an accelerated BDC 15 days prior to SSW wind reversals, and sudden deceleration after the central date.

The present study attempts to examine the question with improved reanalysis products and satellite observations. The current study analyses BDC intensity variation and the resulting stratospheric distribution of ozone. We are using Aura Microwave Limb Sounder (MLS) observations to analyze the stratospheric distribution of ozone. The ERA5 reanalysis products are used to evaluate various metrics to quantify the strength of the circulation.

2. Data

2.1 Aura MLS

The ozone measurements used in the study are from Aura MLS, onboard Aura satellite launched on July 15, 2004. Aura is a near-polar orbiting satellite at 705 km, part of the A-train series [8]. The satellite uses the microwave limb-sounding technique to provide global measurements of several atmospheric species along with temperature and geopotential height.

The satellite carries seven radiometers, from 118 GHz to 2.5 Thz. The 240 GHz radiometer provides the ozone measurements. Water vapor is from the 190 GHz radiometer. The stratospheric ozone mixing ratio from MLS has an accuracy of ~300 ppbv. The water vapor has an accuracy of ~7% in the stratosphere.

2.2 ERA5

The meridional wind, zonal wind, and vertical velocity are taken from the ERA5 reanalysis dataset. Hourly estimates of meteorological parameters are provided by ERA5 with 37 pressure levels. The data set contains atmospheric variables assimilated using the 4D-Var assimilation system [5]. ERA5 is the fifth-generation atmospheric reanalysis from European Centre for Medium-Range Weather Forecasts (ECMWF) providing 1000 hPa to 1 hPa reanalysis products, with higher spatial and temporal resolutions than the previous reanalysis products.

3. Results

3.1 Atmospheric background

The central date of SSW was identified using the World Meteorological Organisation (WMO) definition. Accordingly, the zonal-mean zonal wind at 60°S and at 10 hPa is examined to find the date of reversal of the wind to westward (negative) direction, and it is taken as the central date. The mean temperature is also analyzed at the same pressure level over 65°S to 90°S.

As shown in Fig. 1, the temperature reaches a maximum after September 16, which coincides with a minimum in zonal-mean zonal-wind. However, the wind did not reverse, and hence the 2019 SSW is classified as a minor warming.

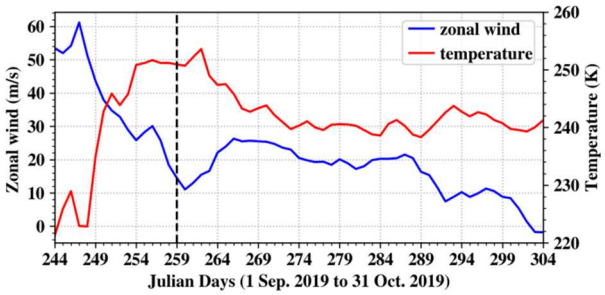

Figure 1. Day evolution of zonal-mean zonal wind at 60° S at 10 hPa and zonal-mean temperature at 10 hPa averaged for latitudes 65°S to 90°S taken from ERA5 reanalysis.

3.2 Diabatic heating rate

The adiabatic ascent associated with the upwelling branch of BDC results in cooled air parcels. The absorption of heat followed can be taken as a measure of the strength of the circulation. Thus, the diabatic heating rate (DHR) is used to measure the intensity of the circulation. DHR is calculated using the following equation;

$$\frac{Q}{c_p} = \frac{\partial T}{\partial t} + v.\nabla T - \omega\left(\frac{\kappa T}{p} - \frac{\partial T}{\partial t}\right) \quad \text{(E1)}$$

Here Q denotes the total heat absorbed, c_p is specific heat capacity, T denotes temperature, p is pressure, v and w are meridional and vertical wind. K is R/c_p, with a value 0.286.

The zonal-mean DHR is averaged from 15°S to 15°N and from 100 hPa to 10 hPa from ERA5 reanalysis. The obtained DHR is shown in figure 2. An increased DHR is observed around SSW central date This results from the enhanced upwelling over the tropical region.

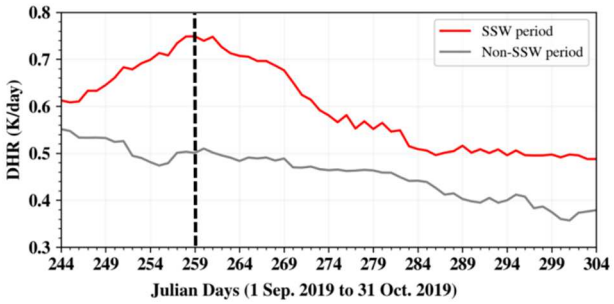

Figure 2. Zonal-mean DHR averaged from 15°S to 15°N and 100 hPa to 10 hPa calculated from ERA-5 reanalysis. DHR spans from September to October during 2019 (red) and 2020 (grey) over the SH.

3.3 Eliassen-Palm flux

The BDC intensity and the driving wave activity are analyzed using various metrics. To quantify the driving force of BDC, Eliassen-Palm (E-P) flux is used. The components of E-P flux are given by;

$$F_\phi = \rho a cos\varphi \overline{u'v'} \quad \text{(E2.a)}$$

$$F_z = f\rho a cos\varphi \frac{\left(\overline{v'\theta'}\right)}{\overline{\theta}_z} \quad \text{(E2.b)}$$

Here the over-bars denote the zonal means and primes denote the deviation from zonal means. ρ is the atmospheric density, φ is the geographical latitude, θ denotes the potential temperature, and the subscript z implies partial derivative with respect to z, the log-pressure height. u and v denote zonal and meridional winds respectively.

The vertical component of E-P flux is scaled by multiplying with 300 for visibility. The E-P flux and its divergence plotted for 10 days before the central date of SSW, on central date, and 10 days after the central date is shown in Fig. 3 (left panel). The E-P flux divergence over the wave-breaking region is around ~1 $ms^{-1}day^{-1}$. The

increased negative values show increased wave breaking in the stratosphere prior to the warming. During the central date also the wave breaking persists. The E-P flux divergence is greatly reduced after 10 days from the central date due to the changed atmospheric conditions hindering the wave propagation. This analysis suggests that the wave activity varies significantly around the SSW period.

3.4 Residual mean meridional stream function

The residual mean meridional stream function (RMMSF) provides an approximation to the mean advective transport of trace substances. RMMSF is calculated from the equation given below;

$$\psi^* = \int_x^{\infty} \overline{v^*} \rho a \cos\varphi \, dz \qquad \text{(E3)}$$

where $\overline{v^*}$ denotes the vertical component of residual velocity and a is the radius of the Earth.

Figure 4 (right panel) shows the) values plotted for central date and 10 days before and after the central date. Before the central date, the latitudinal extent of RMMSF reach a peak. It reduces gradually as SSW progresses. The vertical extent also follows a similar pattern. The magnitude reduces to typical values after the central date. As opposed to this, the polar circulation is observed to be increasing as SSW approaches.

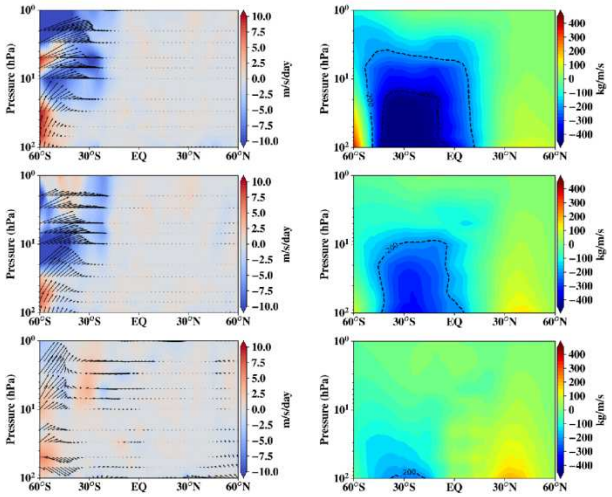

Figure 3. The zonal mean Eliassen-Palm flux (left) and residual mean meridional stream function (right) calculated from ERA-5 reanalysis 10 days before (top), during (middle), and 10 days after (bottom) the central date of SSW.

3.5 Effect of BDC on Ozone

The ozone mixing ratios observed from Aura MLS were used to analyse the stratospheric ozone composition changes during the SSW period. We have taken 60 days of ozone mixing ratios in the southern polar region and over the tropics. The monthly mean was removed from the obtained data. The seasonal mean was removed from the years 2019 and 2020.

A positive ozone anomaly is observed prior to the warming in the tropical upper stratosphere (Fig. 4). The tropical upper stratosphere ozone distribution is strongly affected by photochemical reactions. The nitrogen cycle constitutes ~70% of the ozone destruction over this region, which is strongly linked to temperature [7] The increased upwelling during SSW results in low temperature. The low temperature decreases the efficiency of nitrogen destructive cycle, leading to the observed high ozone concentrations.

In the lower stratosphere reduced ozone mixing ratios are observed around the central date. The enhanced transport could be leading to the reduced ozone mixing ratios.

Over the polar region, a downward propagating positive ozone anomaly is observed during the SSW. The increased downwelling from the upper stratosphere during the warming results in this increased ozone mixing ratio. The polar upper stratosphere shows depleting regions of ozone. This feature could again be attributed to NO_X destructive cycle, where mesospheric air, rich in NO_x comes down into the stratosphere.

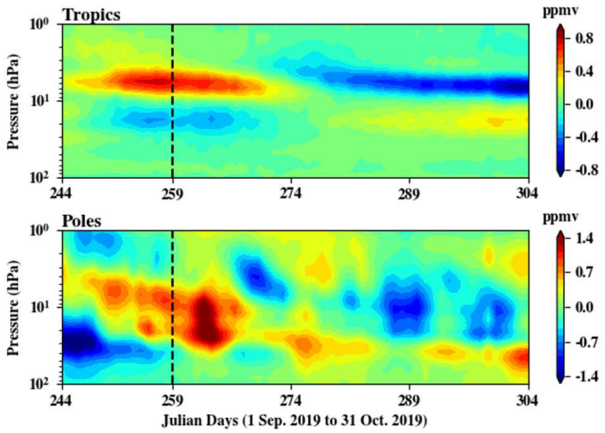

Figure 4. Time evolution of ozone mixing ratio height distribution derived from Aura-MLS for the tropical region (top panel) and polar region (bottom panel).

4. Conclusion

The BDC intensity variation was analyzed during 2019 SSW in the SH. The wave driving is observed to be

increasing around the warming episode, from the divergence of E-P flux. This results in intensified BDC. The increased RMMSF denotes an enhanced circulation that starts before the warming, The latitudinal extent decreases as SSW progresses.

The tropical upper stratosphere ozone shows a positive anomaly around the warming, due to the reduced catalytic destruction rate of the following reaction cycle.

$$\begin{aligned} NO + O_3 &\longrightarrow NO_2 + O_2 \\ NO + O &\longrightarrow NO + O_2 \\ \text{net } O + O_3 &\longrightarrow 2O_2 \end{aligned} \qquad \text{(R1)}$$

The tropical lower stratosphere ozone is reduced around the central date of the warming, this could be due to the enhanced transport by the circulation in the SSW period. In the polar stratosphere, a downward propagating positive ozone anomaly is observed. This is due to the downwelling of ozone-rich air from the upper stratospheric air.

Along with the positive ozone anomaly, regions of ozone depletion are also observed. This is again attributed to the NO_x cycle. In the polar region, NO_x rich mesospheric air intrusion causes the depletion observed during the warming episodes.

The present study has attempted to quantify the changes in stratospheric thermal structure and ozone composition occurring as a result of varying intensity of BDC during Southern Hemisphere SSW.

Acknowledgements

The author Veenus Venugopal thanks the Indian Space Research Organisation for providing a doctoral fellowship during the study period. The authors greatly appreciate the teams of Aura-MLS (https://mls.jpl.nasa.gov) and ECMWF (https://cds.climate.copernicus.eu) for publicly providing the data used in the study.

References

1. Andrews, D. G., Holton, J. R. and Leovy, C. B. “Middle atmosphere dynamics.” International Geophysical Series, Vol. 40, Academic Press, 1987. ISBN: 9780120585762

2. Brewer, A. W. "Evidence for a world circulation provided by the measurements of helium and water vapour distribution in the stratosphere." Quarterly Journal of the Royal Meteorological Society 75, no. 326: 351-363, 1949.. doi:10.1002/qj.49707532603

3.Dobson, G., "Origin and distribution of the polyatomic molecules in the atmosphere." Proceedings of the Royal Society of London. Series A. Mathematical and Physical Sciences 236, no. 1205 (1956): 187-193. doi: 10.1098/rspa.1956.0127

4. de la Cámara, A., M. Abalos, and P. Hitchcock. "Changes in stratospheric transport and mixing during sudden stratospheric warmings." Journal of Geophysical Research: Atmospheres 123, no. 7 (2): 3356-3373, 2018. doi:10.1002/2017JD028007

5. J. R. Holton, P. H. Haynes, M. E. McIntyre, A. R. Douglass, R. B. Rood, and L. Pfister, “Stratosphere-troposphere exchange,” Reviews of Geophysics, vol. 33, no. 4. American Geophysical Union (AGU), p. 403, 1995. doi: 10.1029/95rg02097.

6. K. Kodera, “Influence of stratospheric sudden warming on the equatorial troposphere,” Geophysical Research Letters, vol. 33, no. 6. American Geophysical Union (AGU), 2006. doi: 10.1029/2005gl024510.

7. D. J. Lary, "Catalytic destruction of stratospheric ozone." Journal of Geophysical Research: Atmospheres 102, no. D17: 21515-21526, 1997. doi:10.1029/97JD00912.

8. N. J. Livesey et al., “Investigation and amelioration of long-term instrumental drifts in water vapor and nitrous oxide measurements from the Aura Microwave Limb Sounder (MLS) and their implications for studies of variability and trends,” Atmospheric Chemistry and Physics, vol. 21, no. 20. Copernicus GmbH, pp. 15409–15430, Oct. 15, 2021. doi: 10.5194/acp-21-15409-2021.

9. T. Matsuno, “A Dynamical Model of the Stratospheric Sudden Warming,” Journal of the Atmospheric Sciences, vol. 28, no. 8. American Meteorological Society, pp. 1479–1494, Nov. 1971. doi: 10.1175/1520-0469(1971)028<1479:admots>2.0.co;2.

10. M. Tao, Y. Liu, and Y. Zhang, “Variation in Brewer–Dobson circulation during three sudden stratospheric major warming events in the 2000s,” Advances in Atmospheric Sciences, vol. 34, no. 12. Springer Science and Business Media LLC, pp. 1415–1425, Nov. 08, 2017. doi: 10.1007/s00376-017-6321-1.